Accepted: 4 May 2017

DOI: 10.1111/petr.12986

ORIGINAL ARTICLE

WILEY

Diffuse myocardial fibrosis among healthy pediatric heart transplant recipients: Correlation of histology, cardiovascular magnetic resonance, and clinical phenotype

Brian Feingold[1,2] | Cláudia M. Salgado[3] | Miguel Reyes-Múgica[3] | Stacey E. Drant[1] | Susan A. Miller[1] | Mark Kennedy[4] | Peter Kellman[5] | Erik B. Schelbert[2,4,6] | Timothy C. Wong[4,6]

[1]Department of Pediatrics, University of Pittsburgh School of Medicine, Pittsburgh, PA, USA

[2]Clinical and Translational Science, University of Pittsburgh School of Medicine, Pittsburgh, PA, USA

[3]Department of Pathology, University of Pittsburgh School of Medicine, Pittsburgh, PA, USA

[4]Cardiovascular Magnetic Resonance Center, UPMC Heart and Vascular Institute, Pittsburgh, PA, USA

[5]National Heart Lung and Blood Institute, National Institutes of Health, Bethesda, MD, USA

[6]Department of Medicine, University of Pittsburgh School of Medicine, Pittsburgh, PA, USA

Correspondence
Brian Feingold, MD, MS, Children's Hospital of Pittsburgh of UPMC, Pittsburgh, PA, USA.
Email: brian.feingold@chp.edu

Funding information
American Heart Association/Enduring Hearts, Grant/Award Number: 14GRNT20380101; American Heart Association/Children's Cardiomyopathy Foundation, Grant/Award Number: 14SDG18740035; National Center for Advancing Translational Sciences of the National Institutes of Health, Grant/Award Number: KL2TR000146; National Institutes of Health, Grant/Award Number: UL1-TR-001857

Abstract

Fibrosis is commonly described in heart allografts lost late after transplantation. CMR-derived ECV is a validated measure of DMF in native adult hearts that may predict heart failure and mortality. We explored associations of ECV with histologic myocardial fibrosis and clinical features after pediatric heart transplantation. Twenty-five recipients (7.0±6.3 years at transplant and 10.7±6.5 years post-transplant) were prospectively recruited for CMR and BNP measurement at the time of surveillance biopsy. All had normal ejection fractions and lacked heart failure symptoms. Fibrosis was quantified on biopsy after picrosirius red staining as CVF. ECV was quantified using contemporaneous hematocrit on basal and mid-short-axis slices. ECV was moderately correlated with CVF (r=.47; P=.019). We found no associations of ECV with hemodynamics, ischemic time, time since transplantation, or number of prior biopsies or acute rejections. Compared to healthy non-transplant controls, there was no significant difference in ECV (25.1±3.0 vs 23.7±2.0%, P=.09). Log-transformed BNP was correlated with ECV (recipients: r=.46, P=.02; recipients and controls: r=.45, P=.006). These findings suggest ECV quantifies DMF and relates to biological indicators of cardiac function after pediatric heart transplantation.

KEYWORDS

allograft survival, cardiac magnetic resonance imaging, chronic rejection, extracellular volume, fibrosis, heart transplantation, interstitium, pediatric

Abbreviations: ACE, angiotensin-converting enzyme; AMR, antibody-mediated rejection; BNP, B-type natriuretic peptide; CAV, coronary allograft vasculopathy; CMR, cardiac magnetic resonance; CVF, collagen volume fraction; DMF, diffuse myocardial fibrosis; DSA, donor-specific antibody; ECM, extracellular matrix; ECV, extracellular volume; EMB, endomyocardial biopsy; HLA, human leukocyte antigen; HT, heart transplant; H&E, hematoxylin and eosin; IHC, immunohistochemistry; ISHLT, International Society for Heart and Lung Transplantation; LGE, late gadolinium enhancement; LV, left ventricle; ms, milliseconds; PA, pulmonary artery; PSIR, phase-sensitive inversion recovery; RV, right ventricular; SSFP, steady-state free precession.

1 | INTRODUCTION

Despite improvements in early post-transplant survival, the rate of progression to allograft loss after pediatric HT has not changed since the 1980s.[1] Most late deaths are attributed to "graft failure" and "chronic rejection,"[1] and on histologic analysis, many of these failed allografts are characterized by coronary vasculopathy and fibrosis.[2] CMR-derived ECV fraction is a validated noninvasive measure of DMF in the absence of edema or infiltrative disease.[3] ECV quantifies the full spectrum of myocardial fibrosis and is highly correlated with histologic measures of the CVF (ie, diffuse fibrosis) of the LV in adults.[4-8] ECV is also highly reproducible[6,9-13] and may predict heart failure outcomes and mortality in adults.[14,15] While ECV is a robust metric of DMF, very little has been reported about whether ECV can detect DMF and DMF-associated allograft dysfunction in HT recipients. In this exploratory study, our aims were to validate the association of ECV with histologic myocardial fibrosis in a cohort of prospectively recruited pediatric HT recipients and to explore associations of ECV with clinical indicators of allograft function. We hypothesized that ECV is correlated with histologic myocardial fibrosis, hemodynamics, and serum BNP level.

2 | METHODS

After approval from the University of Pittsburgh Institutional Review Board (PRO13020024), we prospectively enrolled consecutive pediatric HT recipients who were ≥13 years of age for ECV quantification at the time of clinically indicated, surveillance EMB. Because factors besides the accumulation of excess collagen can expand the ECM,[3] recipients with clinically significant acute rejection (≥grade 2R/pAMR1)[16,17] on concurrent EMB were excluded from analysis. We also did not recruit recipients who were <9 months post-HT to reduce the possibility of confounding from ischemia-reperfusion injury that occurs with the HT procedure. Patients who were not able to undergo a complete, contrast-enhanced CMR scan without sedation, including those with glomerular filtration rate ≤30 mL/min/1.73 m^2 or for other reasons (eg, retained pacemaker leads), were not approached for consent. Because normal ECV ranges have not been established across various CMR platforms, we also recruited 12 healthy, non-HT individuals between the ages of 18 and 30 years to serve a comparison group. Individuals with known medical issues, regular medication use, or history of smoking were not enrolled. IRB stipulations did not allow us to enroll individuals aged <18 years to serve as controls for this protocol.

2.1 | CMR scans

CMR scans were performed by dedicated CMR technologists with a 1.5T Siemens Magnetom Espree (Siemens Medical Solutions, Erlangen, Germany) and a 32-channel phased array cardiovascular coil. The examination included standard breath held segmented cine imaging in the short and long axes with SSFP.[18] LV dimensions, myocardial mass (indexed to body surface area), volume indices, and ejection fraction were measured from short-axis stacks of end-diastolic and end-systolic cine frames. LGE imaging[18] was performed 10 minutes after a 0.2 mmol/kg intravenous gadoteridol (Prohance, Bracco Diagnostics, Princeton, NJ, USA) or gadobutrol (Gadavist, Bayer Healthcare Pharmaceuticals, Whippany, NJ, USA), based on clinical availability. To optimize LGE, we used PSIR pulse sequences to increase signal-to-noise ratios, correct for surface coil intensity variation, and render signal intensity proportional to T1 recovery; we used both segmented gradient echo and single-shot SSFP sequences.[19,20] When patients could not breath-hold or had arrhythmia, single-shot SSFP, motion-corrected, averaged PSIR images were acquired.[20,21]

Because native (precontrast) T1 times reflect both intra- and extracellular characteristics of the myocardium, T2 mapping was also performed to determine whether long relaxation times suggestive of myocardial edema were present. T2 mapping was performed prior to contrast administration in the basal and mid-ventricular short-axis orientation, and values were averaged to generate a composite T2 time. Four single-shot images at increasing T2 preparation times (0, 24, 40, and 60 ms, respectively) were acquired according to the following parameters: pixel bandwidth=977 Hz per pixel; echo time=1.2 ms; repetition time ~3.6 ms; flip angle=40°; acquisition matrix=144×256; and slice thickness=6 mm. Following motion correction and pixelwise fitting to estimate T2 relaxation times, a color T2 map was generated.

2.2 | Quantification of the ECV fraction

All CMRs were interpreted by a single investigator (TCW) who was blinded to clinical characteristics, transplant history, EMB findings/fibrosis quantification, and serum biomarker results. We employed methods described previously that yield prognostically relevant, reproducible ECV measures of ECM expansion in adults in non-infarcted myocardium after a gadolinium bolus with minimal variation related to heart rate or time elapsed following the bolus.[12,14,22,23] For native T1, we used two inversion pulses with a 5- and 2-sampling scheme (5+2=7 images total) with two additional dummy heartbeats separating inversion pulses. For post-contrast T1, we employed three inversion pulses with a 4-, 3-, and 2-sampling scheme (4+3+2=9 images total) with one additional dummy heart beat separating inversion pulses. We validated T1 measures using an electrocardiogram-gated, single-shot, modified Look Locker inversion recovery sequence against $CuSO_4$ phantoms with physiological T1 and T2 values for myocardium and blood.[12,14,22,23] We measured the full spectrum of myocardial fibrosis. We did not exclude foci of non-infarcted scar on LGE images (ie, atypical of myocardial infarction) from quantitative ECV measures acquired in non-infarcted myocardium,[14] which would bias ECV measures downwards to an unpredictable extent. We traced the middle third of the myocardium to avoid partial volume effects and quantified ECM expansion with ECV as described previously.[5,14,24,25] Each ECV measurement for a short-axis slice location was derived from a map created using a single native and

corresponding post-contrast T1 measurement occurring after LGE images 19 minutes following the contrast bolus.[26,27] Hematocrit and serum BNP were acquired within 24 hours of the CMR (median 2 hours prior to CMR with interquartile range of 24 minutes before CMR to 4 hours after CMR). We averaged ECV measures from basal and mid-ventricular short-axis slices to yield the final measurement. Apical slices were avoided due to concerns of signal contamination related to partial volume averaging.[28]

2.3 | Histology and quantification of myocardial fibrosis as CVF

From each HT recipient, at least five EMB specimens from the RV apex were obtained using a bioptome during clinically indicated, surveillance catheterization. Specimens were fixed immediately in 10% buffered formalin and embedded in paraffin. Cut sections (5 μm thick) were slide-mounted and stained with hematoxylin and eosin (H&E) for routine clinical assessment and with picrosirius red for fibrosis quantification. Although we excluded recipients with acute rejection on concurrent EMB on the basis that factors besides the accumulation of excess collagen can expand the ECM, slides were also assessed for CD3 and CD163 by IHC to quantify the presence of T lymphocytes and macrophages, respectively. Primary anti-CD3 polyclonal antibody (Dako, Carpinteria, CA, USA) at 1:250 dilution and anti-CD163 monoclonal antibody (clone 10D6; Vector, Burlingame, CA, USA) at 1:250 dilution were used, and IHC was performed on the Benchmark XT IHC automated staining platform (Ventana Medical Systems, Tucson, AZ, USA) following the manufacturer's instructions, with controlled and standardized conditions and positive and negative controls.

All slides were scanned with an Aperio CS2 slide scanner (Leica Biosystems, Buffalo Grove, IL, USA) at 20× magnification, yielding a scan resolution of 0.5 μm per pixel. The accompanying software allows the user to navigate through the captured whole slide image at any digital zoom up to 40×. For each patient, morphometric analysis of the EMB digital image showing one cut section of all biopsy specimens at 10× magnification was performed by a pediatric pathologist (CS) who was blinded to all other data. The analysis used an ImageJ [29] macro to quantify the CVF which is the percentage of stain of interest (eg, picrosirius red) relative to the total amount of myocardium, excluding any areas of technical artifact, endocardium, and pericardium. This methodology is highly correlated with fibrosis quantification by both polarization microscopy and stereology on paraffin-embedded myocardium.[30] EMBs without at least one cut section of myocardium ≥1.5 mm^2 were excluded from analysis.

2.4 | Clinical data

Clinical data abstraction was performed by one investigator (BF) who was blinded to CMR and CVF results. Data abstracted included demographics, transplant characteristics (eg, age at HT, allograft ischemic time, donor age), concurrent EMB rejection grade, and details about presence/timing of CAV, diabetes mellitus, and ACE inhibitor use.

2.5 | Statistical analysis

Categorical variables are presented as count (percentage) and continuous variables as mean±standard deviation (and range). Comparisons of categorical variables were made using Fisher's exact test and continuous variables using the Wilcoxon rank-sum test. Correlations were assessed using Pearson's correlation coefficient. Continuous variables with a skewed distribution were log-transformed for correlation analysis if transformation resolved skewedness. ECVs derived in HT patients who received gadoteridol were compared to those who received gadobutrol. Unless otherwise noted, all statistical tests are two-sided and $P<.05$ was considered significant. Study data were collected and managed using REDCap (Research Electronic Data Capture) tools hosted at the University of Pittsburgh Clinical and Translational Science Institute. REDCap is a secure, web-based application designed to support data capture for research studies.[31] Statistical analyses were performed using Stata v14.1 (StataCorp, College Station, TX, USA).

3 | RESULTS

Thirty-one HT recipients underwent paired CMR and EMB. Three recipients were excluded from analysis due to concurrent acute rejection on EMB and three were excluded prior to any CMR post-processing because of motion artifact in a thin-walled (~5 mm) ventricle (n=2) and operator error in pulse sequence specification (n=1). Demographic features of the 25 HT recipients included in the analysis are shown in Table 1 and clinical findings at paired CMR-EMB are shown in Table 2. The cohort was

TABLE 1 HT recipient demographics

	HT recipients (n=25)
Female	6 (24)
Race	
Caucasian	24 (96)
Black	1 (4)
Asian	0 (0)
Age at CMR (y)	17.7±2.9 (13.2-26)
Age at HT (y)	7.0±6.3 (0-16.5)
Time from HT to CMR (y)	10.7±6.5 (0.9-24.8)
Allograft age at CMR (y)	18.0±3.8 (13.7-28.8)
Graft ischemic time at HT (min)	211.4±73.0 (104-467)
Positive donor-specific cross-match	0 (0)
History of diabetes mellitus	2 (8)
Any post-HT use of ACE inhibitor	10 (40)
Number of prior EMB procedures	23.9±10.5 (1-49)
Maintenance immunosuppression	
Tacrolimus/Cyclosporine	24 (96)/1 (4)
Mycophenolate mofetil	17 (68)
Prednisone	6 (24)
Sirolimus	2 (8)
Azathioprine	1 (4)

TABLE 2 Clinical findings at paired CMR-EMB among HT recipients

EMB acute rejection grade	
0	21 (84)
1R	4 (16)
Serum DSA present[a]	3 (13)
Graft vasculopathy	4 (16)
Hemodynamics	
Right atrium (mm Hg)	4.1±1.9 (1-8)
PA wedge pressure (mm Hg)	7.6±2.7 (4-14)
Cardiac index (mL/min/m^2)	3.6±0.7 (2.3-5.2)
CMR indices	
Ejection fraction (%)	59.6±5.5 (51-70)
LV end-diastolic volume (mL/m^2)	70.9±11.4 (48.4-86.5)
LV end-systolic volume (mL/m^2)	28.7±6.7 (18.8-41.9)
LV mass (g/m^2)	44.2±7.7 (30.7-58.3)
BNP (pg/mL)	48.6±42.8 (4-212)

PA, pulmonary artery.
[a]n=23 (in two recipients, HLA antibody was present but DSA determination could not be made).

generally healthy from a cardiovascular perspective with normal filling pressures, cardiac index, ejection fraction and other routine CMR parameters, and serum BNP level (Table 2). Three recipients each had a single HLA class I DSA of weak to moderate mean fluorescence intensity with two other patients each having a single HLA antibody for which donor specificity could not be determined due to the remoteness of their HT. The four recipients with known CAV at the time of CMR had minimal diminishment of distal vessels without epicardial disease (ISHLT CAV1). In these recipients, CAV diagnosis was made 8.3-10.2 years prior to CMR.

Blinded histologic analysis revealed median CVF of 2.4% (0.6%-5.9%). The median proportions of CD3 (T lymphocytes) and CD163 (macrophage) staining on EMB specimens were low at 0.2% (0.0%-1.8%) and 0.2% (0.3%-1.8%), respectively, consistent with the exclusion of recipients with acute rejection. EMB obtained at the time of CMR was inadequate (total myocardial area <1.5 mm^2) in two HT recipients, and in these cases, the most recent prior EMB (obtained 5 months and 1 year prior) was used. Figure 1 shows representative histology findings on H&E, picrosirius red, CD3, and CD163 of a single EMB specimen.

As shown in Figure 2, ECV was moderately correlated with CVF (r=.47, P=.019) and log-transformed serum BNP in HT recipients (r=.46; P=.022) and among HT recipients and controls (r=.45; P=.006). We

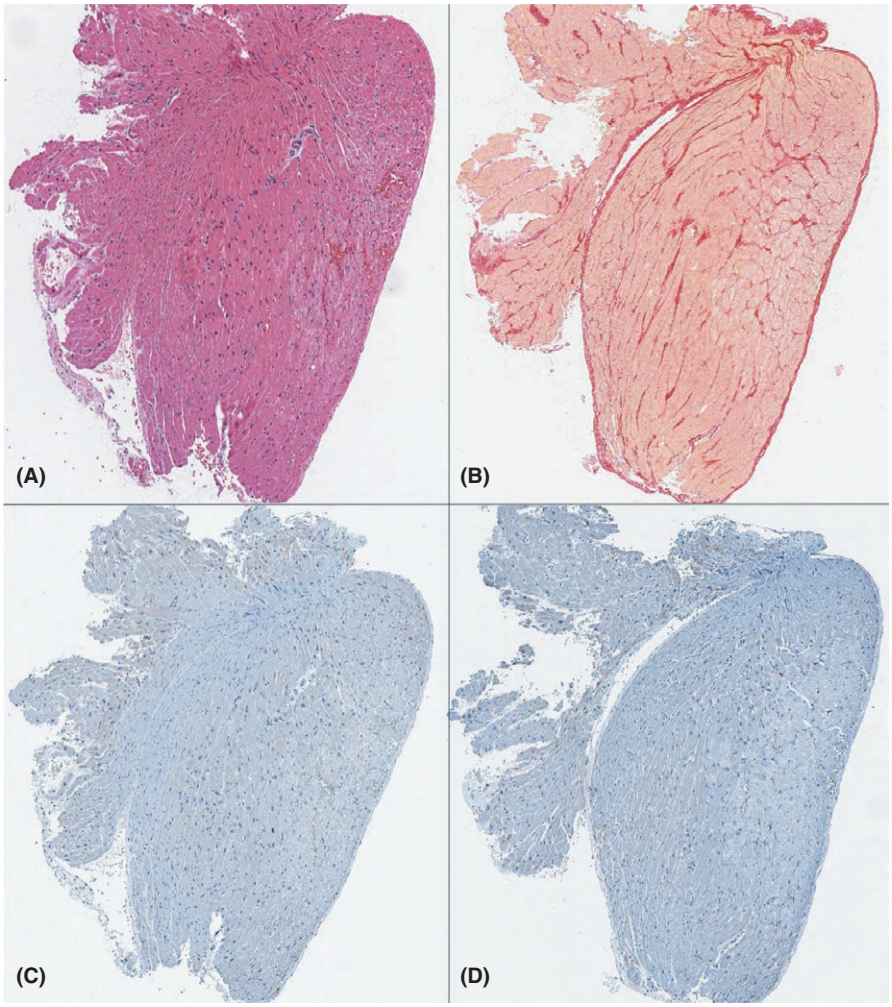

FIGURE 1 Representative histology findings on (A) H&E, (B) picrosirius red to highlight collagen, (C) CD3 for T lymphocytes, and (D) CD163 for macrophages of a single EMB specimen (magnification 6.8×)

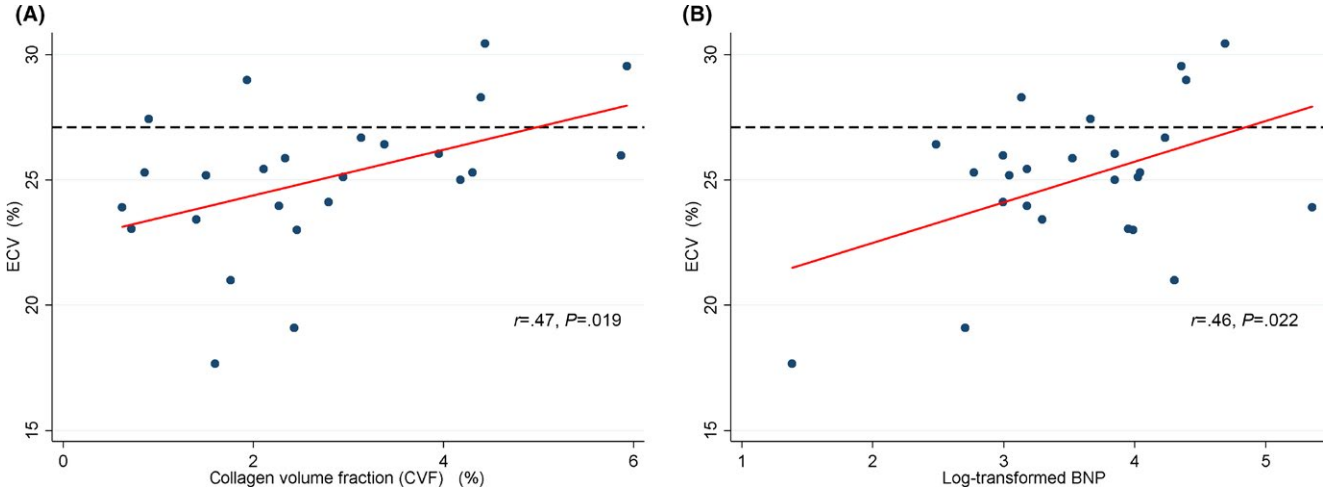

FIGURE 2 Scatterplots showing the linear correlation of ECV with (A) % fibrosis by EMB (picrosirius red staining) and (B) log-transformed serum BNP level. The horizontal dashed line depicts the upper limit of ECV in our healthy non-HT cohort (aged 18-25 y)

found no associations of ECV with CD3 or CD163, hemodynamics, allograft ischemic time, time after transplantation, allograft age, or number of prior EMBs or acute rejection events (Table 3). Exclusion of the two cases where the prior EMB was analyzed (concurrent EMB area too small for analysis) did not alter any of the correlation analyses results, including ECV with CVF (r=.49, P=.017) and log-BNP (r=.46, P=.028).

Among HT recipients, there were no significant differences in ECV on the basis of female sex (26.2±1.5% vs 24.7±3.2%, P=.31), history of ACE inhibitor use (24.3±3.2% vs 25.5±2.9%; P=.15), history of acute cellular rejection ≥grade 2R in the first post-HT year (25.6±3.1% vs 24.6±3.1%, P=.45) or at any time prior to CMR (25.7±2.9% vs 23.7±3.2%, P=.23), presence of DSA at CMR (26.3±3.8% vs 24.9±3.0%, P=.72), or CAV (25.6±2.9% vs 24.9±3.0%, P=.94). Atypical LGE (ie, not associated with coronary distribution) was observed in two HT recipients: One had scant elevated signal at the inferior RV insertion point and the other showed a punctate focus of midwall signal in the apical inferior wall. ECVs were 25.9% and 26.0%, respectively.

TABLE 3 ECV correlations among HT recipients

Variable	*r*	*P*-value
Histologic myocardial fibrosis	.47	**.019**
CD3	−.19	.37
CD163	−.03	.90
Log BNP	.46	**.022**
Mean right atrium pressure	−.02	.91
Mean PA wedge pressure	.22	.29
Cardiac index	.38	.07
Ischemic time	.11	.60
Time after HT	.03	.90
Allograft age	−.06	.80
Number of prior EMBs	.13	.54
Number of prior acute rejections	.27	.21

PA, pulmonary artery.

Representative raw images and ECV maps of HT recipients and healthy, non-HT controls are shown in Figure 3. There was no significant difference in ECV between HT recipients and controls (25.1±3.0% vs 23.7±2.0%, P=.09). Five HT recipients (20%) had ECV >27.1%, the upper limit observed in the healthy, non-HT control group. Comparison of ECV among HT recipients according to contrast agent showed no difference (25.1±3.2 vs 25.0±2.6, P=.5).

Because myocardial native T1 values are sometimes used for DMF quantification, we measured this and found no difference between HT recipients and healthy, non-HT controls (1019±25 vs 1016±28 ms, P=.52). Further, native T1 was neither correlated with CVF (r=.12, P=.58) nor log-transformed BNP in HT recipients (r=.05, P=.81) or recipients and controls (r=.05, P=.8). Also, when we analyzed ECV and native T1 values limited to only the interventricular septum, we found a trend to higher septal ECV for HT recipients (26.2±3.4%) vs controls (24.4±2.2%, P=.06) with no difference in septal native T1 values (1027±30 vs 1024±32, P=.67) between the groups. Among HT recipients, correlations of septal ECV with CVF (r=.51, P=.01) and log-BNP (r=.45, P=.03) were similar to correlations of ECV from the entire LV (Table 3). There were no correlations of septal native T1 (r=.21, P=.31) with CVF or log-BNP (r=.14, P=.51). Also, we observed no correlations of septal ECV or native T1 with ischemic time, time after HT, allograft age, or number of prior EMBs or acute rejection events. Short-axis T2 times among transplant recipients were not higher than those from healthy, non-HT controls (one-sided P>.9).

4 | DISCUSSION

In this study, we report novel moderate correlations of ECV with histologic fibrosis on RV EMB and serum BNP in a healthy cohort of adolescents and young adults who received HT during childhood. ECV was not associated with time since HT, allograft age, or number of prior acute rejection events. These findings suggest that ECV reflects the quantity of DMF after pediatric HT in the absence of HF

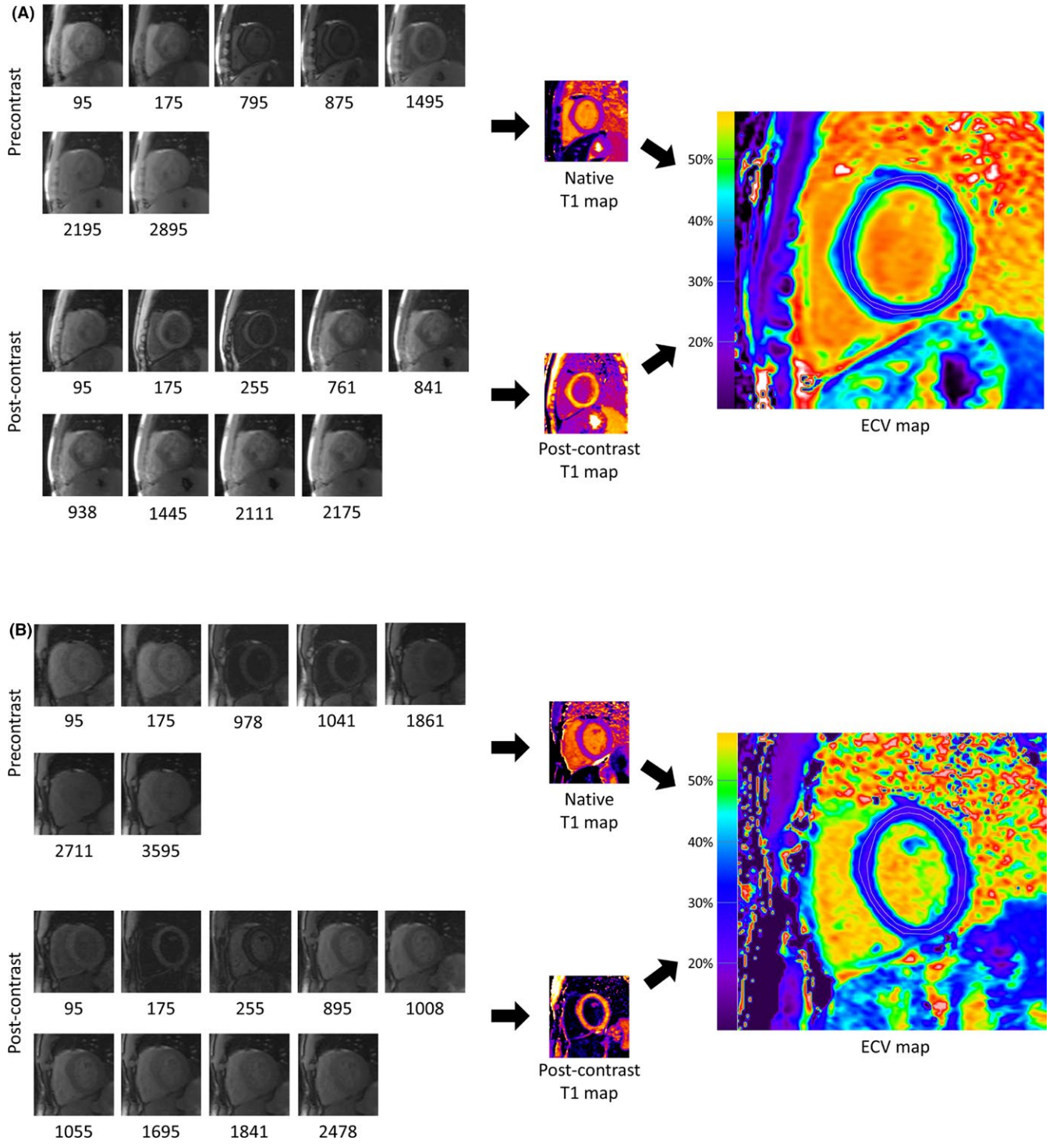

FIGURE 3 Representative raw CMR images and ECV maps of HT recipients (A) and healthy, young adult, non-HT controls (B)

symptomatology or clinically evident allograft dysfunction and that is otherwise not predicted by time after HT, number of prior EMBs, or rejection history. The correlation of ECV with serum BNP that we observed in the HT recipients supports the concept that DMF adversely impacts allograft health. There is a growing body of literature in non-HT adult HF populations that identifies DMF as a detrimental, common response pathway arising from a variety of insults.[32-34] Evidence to support a link between DMF and adverse HT outcomes is less well established, particularly in pediatric HT recipients where reports are extremely sparse.[35] Data from animal models and studies of adult HT recipients show that immune responses against allograft endothelial antigens and antigen-independent insults result in fibrotic remodeling of the allograft.[36-38] Whether there is overlap between the downstream mediators of DMF of the cardiac allograft and the non-transplanted heart is uncertain. Both transforming growth factor-beta and interleukin-6 have been associated with allograft fibrosis[39,40]

and also with non-transplant cardiac fibrosis,[41] suggesting there may be a common final pathway to interstitial myocardial fibrosis, regardless of the triggering event.

Published data on CMR quantification of myocardial fibrosis after HT are very limited and have used a variety of methodologies, including native T1 mapping, post-contrast T1 mapping, and ECV.[42-45] In the most pertinent study, Ide et al.[45] found greater ECV and native T1 values among 20 pediatric HT recipients relative to non-HT controls. They also reported moderate correlations of ECV (r=.46) and native T1 values (r=.53) of the interventricular septum (but not the entire LV) with CVF, and that septal native T1 was moderately correlated (r=.46) with ischemic time. Many of these findings, including the septal, but not entire LV ECV correlation with CVF, and all native T1 correlations are different than ours. While the relatively small numbers of participants in both studies may underlie some of the differences, the Ide et al. cohort was younger (9.9±6.2 years), earlier out from HT (median 1.3 years, range 0.02-12.6 years with four recipients at <90 days post-HT), had greater prevalence of mild acute rejection at the time of CMR (11/20), and had higher CVF (10.0±3.4%) than our HT cohort. Their inclusion of recipients early out from HT may have confounded native T1 and ECV measurements due to myocyte and extracellular edema from allograft ischemia-reperfusion injury,[46] potentially exaggerating differences in ECV and native T1 between HT recipients and controls and contributing to the correlation of ischemic time with native T1 observed in their study. Also the difference in CVF between studies deserves mention as it may explain the similar ECV yet dissimilar native T1 correlations with CVF observed. Among hearts with more DMF (CVF ~10%) in the Ide et al. study, both ECV and native T1 correlated with CVF, whereas with less fibrosis (~2.5%) we observed only ECV correlated with CVF. Thus ECV may represent the more sensitive indicator of DMF and is consistent with the fact that native T1 reflects myocardial disease involving the myocyte and extracellular space whereas ECV estimates only the extracellular space.[3]

Among other studies of CMR quantification of myocardial fibrosis after HT, Iles et al. showed that ECV and post-contrast T1 time correlated with LV stiffness in adult HT recipients (median of 39 months post-HT, 35% with exertional dyspnea), supporting a link between DMF and diastolic dysfunction.[42] Although we did not find an association of ECV with ventricular filling pressures in our cohort, we did find ECV correlated with BNP levels, a marker of both systolic and diastolic dysfunction.[47,48] It is also worth noting that histologic validation studies of CMR-quantified fibrosis in adult native hearts generally show stronger correlations than we observed. However, nearly all of these studies assessed LV histology on tissue that was obtained by surgical or core-needle biopsy of adults with symptomatic heart failure, aortic stenosis, or hypertrophic cardiomyopathy.[4-8,49-54] In contrast, we assessed histology using RV EMB samples, which are generally smaller and more confined to the subendocardium as compared to direct-visualization core-needle or excisional assessments of the LV. This may explain the decreased magnitude of our ECV-CVF association as compared with previously reported correlations in adult native hearts. In addition to the similar moderate correlation of ECV with CVF on RV EMB found by Ide et al. in their post-HT cohort, our data are also similar to two published analyses of CMR-quantified DMF with RV EMB specimen-quantified fibrosis.[43,55]

Moving forward, our data suggest a need for examination of the role of ECV in larger, multicenter cohorts representing the entire disease severity spectrum in order to 1) confirm high ECV in allografts which are failing, and 2) demonstrate the association between ECV and prognosis following pediatric HT. We hypothesize that longitudinal assessments in a larger cohort that includes recipients with clinical heart failure and/or abnormal hemodynamics not due to acute rejection will strengthen the associations we have observed and also allow for determination of the prognostic abilities of ECV after HT. The ability to detect ECV progression before overt clinical findings (eg, elevated filling pressures, decreased ejection fraction, symptomatic heart failure) are present could offer opportunities to study DMF as a risk factor for allograft loss and design interventions aimed at slowing or reversing progression.

There are important limitations of our study. Our cohort was relatively healthy, as demonstrated by low BNP values, normal group mean filling pressures, minimal presence of donor-specific antibodies, low prevalence of CAV, and normal clinical evaluations with no symptoms of heart failure. While most BNPs we observed were normal, data from the adult HT population show prognostic relevance of BNP reported values across a similar range.[56,57] Because most of our cohort received HT more than 10 years ago, the clinical biopsy reports lack sufficient detail to allow us to explore possible associations of ECV with antibody-mediated rejection history. Also, ethical considerations prohibited the use of intravenous contrast in otherwise healthy children, resulting in our non-HT control group being comprised of young adults (ages 18-30 years) rather than age-matched peers. Although increases in ECV with age have been demonstrated among middle-aged adults, the magnitude of this effect was shown to be approximately 0.5%-1% per decade of age and thus would be unlikely to influence our analysis.[25,58] The use of two different contrast agents during the study was unavoidable due to a change in contrast agent selection for clinical CMR scans at our center during the study period. However, we found no difference in ECV on the basis of contrast agent use, a finding that is consistent with an analysis that compared gadoteridol and gadobutrol in a large-scale, prospective clinical neuroimaging study.[59]

Other important considerations of the application of ECV assessment to post-HT populations include retained pacemaker leads or other CMR-incompatible objects, which may exclude some from being able to undergo CMR. In our experience, most children and young adult HT recipients do not have such materials, unlike their adult counterparts who more commonly receive defibrillators or resynchronization therapy prior to transplantation. Finally, it is important to recognize that it may not be possible to measure ECV in some recipients who are late out after HT who also have severe renal impairment (glomerular filtration rate <30 mL/min/1.73 m^2). This is a known complication seen in about 3%-5% of pediatric HT recipients.[60]

In summary, we demonstrate a novel association of ECV with histologic myocardial fibrosis and serum BNP after pediatric HT. These findings show that myocardial fibrosis is quantifiable by noninvasive CMR and may relate to fundamental markers of cardiac function, even in a healthy HT cohort without rejection and with normal clinical

cardiac imaging. Further studies to characterize the role of fibrosis across the entire disease spectrum are warranted.

ACKNOWLEDGMENTS

The authors wish to acknowledge and thank the following individuals for their assistance in completing this research: Kathy Puntil, Deborah Yasko, Elizabeth Ruhl, Stephen Mancuso, and Marie-Therese Najjar of the UPMC CMR Center; and Kelli Smith, Margaret Abraham, and Jane Luce at Children's Hospital of Pittsburgh of UPMC. We also thank all the participants who volunteered their time for this study. This work was supported by funding to BF from the National Center for Advancing Translational Sciences of the National Institutes of Health (award number KL2TR000146) and the American Heart Association and Enduring Hearts (14GRNT20380101). TW's effort was supported in part by the American Heart Association and the Children's Cardiomyopathy Foundation (14SDG18740035). REDCap support was provided by the National Institutes of Health (UL1-TR-001857). No funding body had a role in the design, collection, analysis or interpretation of the data, manuscript composition, or decision to submit for publication.

AUTHORS' CONTRIBUTIONS

Brian Feingold: Conceptualized and planned the research, recruited participants, collected and analyzed data, prepared the manuscript, and critically reviewed the manuscript; Cláudia M. Salgado and Miguel Reyes-Múgica: Conceptualized histology research, performed blinded histologic data analysis, and critically reviewed the manuscript; Stacey Drant: Conceptualized imaging aspects, blinded data analysis, and performed critical review; Susan A. Miller: Recruited participants, collected/analyzed data, and performed critical review; Mark Kennedy: Blindly analyzed CMR data and critically reviewed the manuscript; Peter Kellman: Technical implementation of CMR pulse sequences and ECV maps, blinded quality control review of data, and critically reviewed the manuscript; Erik B. Schelbert: Served as a content expert for ECV, blinded quality control review of data, and critically reviewed the manuscript; Timothy C. Wong: Conceptualized and planned the research, collected and blindly analyzed CMR data, prepared the manuscript, and critically reviewed the manuscript.

REFERENCES

1. Dipchand AI, Kirk R, Edwards LB, et al. The Registry of the International Society for Heart and Lung Transplantation: sixteenth official pediatric heart transplantation report–2013; focus theme: age. *J Heart Lung Transplant*. 2013;32:979-988.
2. Billingham ME. The postsurgical heart. The pathology of cardiac transplantation. *Am J Cardiovasc Pathol*. 1988;1:319-334.
3. Moon JC, Messroghli DR, Kellman P, et al. Myocardial T1 mapping and extracellular volume quantification: a Society for Cardiovascular Magnetic Resonance (SCMR) and CMR Working Group of the European Society of Cardiology consensus statement. *J Cardiovasc Magn Reson*. 2013;15:92.
4. Aus Dem Siepen F, Buss SJ, Messroghli D, et al. T1 mapping in dilated cardiomyopathy with cardiac magnetic resonance: quantification of diffuse myocardial fibrosis and comparison with endomyocardial biopsy. *Eur Heart J Cardiovasc Imaging*. 2015;16:210-216.
5. Flett AS, Hayward MP, Ashworth MT, et al. Equilibrium contrast cardiovascular magnetic resonance for the measurement of diffuse myocardial fibrosis: preliminary validation in humans. *Circulation*. 2010;122:138-144.
6. Fontana M, White SK, Banypersad SM, et al. Comparison of T1 mapping techniques for ECV quantification. Histological validation and reproducibility of ShMOLLI versus multibreath-hold T1 quantification equilibrium contrast CMR. *J Cardiovasc Magn Reson*. 2012;14:88.
7. Miller CA, Naish JH, Bishop P, et al. Comprehensive validation of cardiovascular magnetic resonance techniques for the assessment of myocardial extracellular volume. *Circ Cardiovasc Imaging*. 2013;6:373-383.
8. White SK, Sado DM, Fontana M, et al. T1 mapping for myocardial extracellular volume measurement by CMR: bolus only versus primed infusion technique. *JACC Cardiovasc Imaging*. 2013;6:955-962.
9. Chin CW, Semple S, Malley T, et al. Optimization and comparison of myocardial T1 techniques at 3T in patients with aortic stenosis. *Eur Heart J Cardiovasc Imaging*. 2014;15:556-565.
10. Kawel N, Nacif M, Zavodni A, et al. T1 mapping of the myocardium: intra-individual assessment of post-contrast T1 time evolution and extracellular volume fraction at 3T for Gd-DTPA and Gd-BOPTA. *J Cardiovasc Magn Reson*. 2012;14:26.
11. Liu S, Han J, Nacif MS, et al. Diffuse myocardial fibrosis evaluation using cardiac magnetic resonance T1 mapping: sample size considerations for clinical trials. *J Cardiovasc Magn Reson*. 2012;14:90.
12. Schelbert EB, Testa SM, Meier CG, et al. Myocardial extravascular extracellular volume fraction measurement by gadolinium cardiovascular magnetic resonance in humans: slow infusion versus bolus. *J Cardiovasc Magn Reson*. 2011;13:16.
13. Singh A, Horsfield MA, Bekele S, Khan JN, Greiser A, McCann GP. Myocardial T1 and extracellular volume fraction measurement in asymptomatic patients with aortic stenosis: reproducibility and comparison with age-matched controls. *Eur Heart J Cardiovasc Imaging*. 2015;16:763-770.
14. Wong TC, Piehler K, Meier CG, et al. Association between extracellular matrix expansion quantified by cardiovascular magnetic resonance and short-term mortality. *Circulation*. 2012;126:1206-1216.
15. Wong TC, Piehler KM, Kang IA, et al. Myocardial extracellular volume fraction quantified by cardiovascular magnetic resonance is increased in diabetes and associated with mortality and incident heart failure admission. *Eur Heart J*. 2014;35:657-664.
16. Berry GJ, Burke MM, Andersen C, et al. The 2013 International Society for Heart and Lung Transplantation Working Formulation for the standardization of nomenclature in the pathologic diagnosis of antibody-mediated rejection in heart transplantation. *J Heart Lung Transplant*. 2013;32:1147-1162.
17. Stewart S, Winters GL, Fishbein MC, et al. Revision of the 1990 working formulation for the standardization of nomenclature in the diagnosis of heart rejection. *J Heart Lung Transplant*. 2005;24:1710-1720.
18. Kramer CM, Barkhausen J, Flamm SD, Kim RJ, Nagel E. Standardized cardiovascular magnetic resonance (CMR) protocols 2013 update. *J Cardiovasc Magn Reson*. 2013;15:91.
19. Kellman P, Arai AE, McVeigh ER, Aletras AH. Phase-sensitive inversion recovery for detecting myocardial infarction using gadolinium-delayed hyperenhancement. *Magn Reson Med*. 2002;47:372-383.
20. Ledesma-Carbayo MJ, Kellman P, Hsu LY, Arai AE, McVeigh ER. Motion corrected free-breathing delayed-enhancement imaging of myocardial infarction using nonrigid registration. *J Magn Reson Imaging*. 2007;26:184-190.
21. Piehler KM, Wong TC, Puntil KS, et al. Free-breathing, motion-corrected late gadolinium enhancement is robust and extends risk stratification to vulnerable patients. *Circ Cardiovasc Imaging*. 2013;6:423-432.
22. Messroghli DR, Greiser A, Frohlich M, Dietz R, Schulz-Menger J. Optimization and validation of a fully-integrated pulse sequence for

modified look-locker inversion-recovery (MOLLI) T1 mapping of the heart. *J Magn Reson Imaging*. 2007;26:1081-1086.
23. Xue H, Shah S, Greiser A, et al. Motion correction for myocardial T1 mapping using image registration with synthetic image estimation. *Magn Reson Med*. 2012;67:1644-1655.
24. Lee JJ, Liu S, Nacif MS, et al. Myocardial T1 and extracellular volume fraction mapping at 3 tesla. *J Cardiovasc Magn Reson*. 2011;13:75.
25. Ugander M, Oki AJ, Hsu LY, et al. Extracellular volume imaging by magnetic resonance imaging provides insights into overt and subclinical myocardial pathology. *Eur Heart J*. 2012;33:1268-1278.
26. Kellman P, Wilson JR, Xue H, et al. Extracellular volume fraction mapping in the myocardium, part 2: initial clinical experience. *J Cardiovasc Magn Reson*. 2012;14:64.
27. Kellman P, Wilson JR, Xue H, Ugander M, Arai AE. Extracellular volume fraction mapping in the myocardium, part 1: evaluation of an automated method. *J Cardiovasc Magn Reson*. 2012;14:63.
28. Giri S, Chung YC, Merchant A, et al. T2 quantification for improved detection of myocardial edema. *J Cardiovasc Magn Reson*. 2009;11:56.
29. Rasband WS. *ImageJ*. Bethesda, MD: National Institutes of Health; 2014.
30. Hadi AM, Mouchaers KT, Schalij I, et al. Rapid quantification of myocardial fibrosis: a new macro-based automated analysis. *Cell Oncol (Dordr)*. 2011;34:343-354.
31. Harris PA, Taylor R, Thielke R, Payne J, Gonzalez N, Conde JG. Research electronic data capture (REDCap)–a metadata-driven methodology and workflow process for providing translational research informatics support. *J Biomed Inform*. 2009;42:377-381.
32. Heling A, Zimmermann R, Kostin S, et al. Increased expression of cytoskeletal, linkage, and extracellular proteins in failing human myocardium. *Circ Res*. 2000;86:846-853.
33. Maisch B. Ventricular remodeling. *Cardiology*. 1996;87(Suppl 1):2-10.
34. Sun Y, Weber KT. Cardiac remodelling by fibrous tissue: role of local factors and circulating hormones. *Ann Med*. 1998;30(Suppl 1):3-8.
35. Perens G, Li F, Meier S, Kaur R, Alejos JC, Fishbein M. Clinicopathologic findings in end-stage pediatric heart transplant grafts. *Pediatr Transplant*. 2009;13:887-891.
36. Hornick P, Rose M. Chronic rejection in the heart. *Methods Mol Biol*. 2006;333:131-144.
37. Libby P, Pober JS. Chronic rejection. *Immunity*. 2001;14:387-397.
38. Mannon RB. Therapeutic targets in the treatment of allograft fibrosis. *Am J Transplant*. 2006;6:867-875.
39. Booth AJ, Csencsits-Smith K, Wood SC, Lu G, Lipson KE, Bishop DK. Connective tissue growth factor promotes fibrosis downstream of TGFbeta and IL-6 in chronic cardiac allograft rejection. *Am J Transplant*. 2010;10:220-230.
40. Csencsits K, Wood SC, Lu G, et al. Transforming growth factor beta-induced connective tissue growth factor and chronic allograft rejection. *Am J Transplant*. 2006;6:959-966.
41. Brown RD, Ambler SK, Mitchell MD, Long CS. The cardiac fibroblast: therapeutic target in myocardial remodeling and failure. *Annu Rev Pharmacol Toxicol*. 2005;45:657-687.
42. Ellims AH, Shaw JA, Stub D, et al. Diffuse myocardial fibrosis evaluated by post-contrast t1 mapping correlates with left ventricular stiffness. *J Am Coll Cardiol*. 2014;63:1112-1118.
43. Iles L, Pfluger H, Phrommintikul A, et al. Evaluation of diffuse myocardial fibrosis in heart failure with cardiac magnetic resonance contrast-enhanced T1 mapping. *J Am Coll Cardiol*. 2008;52:1574-1580.
44. Riesenkampff E, Chen CK, Kantor PF, et al. Diffuse myocardial fibrosis in children after heart transplantations: a magnetic resonance T1 mapping study. *Transplantation*. 2015;99:2656-2662.
45. Ide S, Riesenkampff E, Chiasson DA, et al. Histological validation of cardiovascular magnetic resonance T1 mapping markers of myocardial fibrosis in paediatric heart transplant recipients. *J Cardiovasc Magn Reson*. 2017;19:10.
46. Verma S, Fedak PWM, Weisel RD, et al. Fundamentals of reperfusion injury for the clinical cardiologist. *Circulation*. 2002;105:2332-2336.
47. Lubien E, DeMaria A, Krishnaswamy P, et al. Utility of B-natriuretic peptide in detecting diastolic dysfunction: comparison with Doppler velocity recordings. *Circulation*. 2002;105:595-601.
48. Tsutamoto T, Wada A, Maeda K, et al. Attenuation of compensation of endogenous cardiac natriuretic peptide system in chronic heart failure: prognostic role of plasma brain natriuretic peptide concentration in patients with chronic symptomatic left ventricular dysfunction. *Circulation*. 1997;96:509-516.
49. Bull S, White SK, Piechnik SK, et al. Human non-contrast T1 values and correlation with histology in diffuse fibrosis. *Heart*. 2013;99:932-937.
50. de Meester de Ravenstein C, Bouzin C, Lazam S, et al. Histological Validation of measurement of diffuse interstitial myocardial fibrosis by myocardial extravascular volume fraction from Modified Look-Locker imaging (MOLLI) T1 mapping at 3 T. *J Cardiovasc Magn Reson*. 2015;17:48.
51. Iles LM, Ellims AH, Llewellyn H, et al. Histological validation of cardiac magnetic resonance analysis of regional and diffuse interstitial myocardial fibrosis. *Eur Heart J Cardiovasc Imaging*. 2015;16:14-22.
52. Kammerlander AA, Marzluf BA, Zotter-Tufaro C, et al. T1 mapping by CMR imaging: from histological validation to clinical implication. *JACC Cardiovasc Imaging*. 2016;9:14-23.
53. Lee SP, Lee W, Lee JM, et al. Assessment of diffuse myocardial fibrosis by using MR imaging in asymptomatic patients with aortic stenosis. *Radiology*. 2015;274:359-369.
54. Mascherbauer J, Marzluf BA, Tufaro C, et al. Cardiac magnetic resonance postcontrast T1 time is associated with outcome in patients with heart failure and preserved ejection fraction. *Circ Cardiovasc Imaging*. 2013;6:1056-1065.
55. Sibley CT, Noureldin RA, Gai N, et al. T1 Mapping in cardiomyopathy at cardiac MR: comparison with endomyocardial biopsy. *Radiology*. 2012;265:724-732.
56. Martinez-Dolz L, Almenar L, Hervas I, et al. Prognostic relationship between two serial determinations of B-type natriuretic peptide and medium-long-term events in heart transplantation. *J Heart Lung Transplant*. 2008;27:735-740.
57. Martinez-Dolz L, Almenar L, Moro J, et al. Prognostic value of brain natriuretic peptide in heart transplant patients. *J Heart Lung Transplant*. 2007;26:986-991.
58. Liu CY, Liu YC, Wu C, et al. Evaluation of age-related interstitial myocardial fibrosis with cardiac magnetic resonance contrast-enhanced T1 mapping: MESA (Multi-Ethnic Study of Atherosclerosis). *J Am Coll Cardiol*. 2013;62:1280-1287.
59. Kanal E, Maravilla K, Rowley HA. Gadolinium contrast agents for CNS imaging: current concepts and clinical evidence. *AJNR Am J Neuroradiol*. 2014;35:2215-2226.
60. Feingold B, Zheng J, Law YM, et al. Risk factors for late renal dysfunction after pediatric heart transplantation: a multi-institutional study. *Pediatr Transplant*. 2011;15:699-705.

How to cite this article: Feingold B, Salgado CM, Reyes-Múgica M, et al. Diffuse myocardial fibrosis among healthy pediatric heart transplant recipients: Correlation of histology, cardiovascular magnetic resonance, and clinical phenotype. *Pediatr Transplant*. 2017;21:e12986. https://doi.org/10.1111/petr.12986